Wind and Structures, Vol. 3, No. 2 (2000) 97-115
DOI: http://dx.doi.org/10.12989/was.2000.3.2.097

Aspects of the use of proper orthogonal decomposition of surface pressure fields

C.J. Baker†

School of Civil Engineering, University of Birmingham, Edgbaston, Birmingham B15 2TT, U.K.

Abstract. The technique of proper orthogonal decomposition is potentially useful in specifying the fluctuating surface pressure field around structures. However there has been a degree of controversy over whether or not the calculated modes have physical meanings. This paper addresses this issue through consideration of the results of full scale experiments, and through an analytical investigation. It is concluded that the lower, most energetic modes are likely to reflect different fluctuating flow mechanisms, although no mode is likely to be associated with just one flow mechanism or vice versa. The higher, less energetic modes are likely to represent interactions between different flow mechanisms, and to be significantly affected by the number of measurement points and measurement errors. The paper concludes with a brief description of the application of POD to the problem of building ventilation, and the calculation of cladding pressures.

Key words: proper orthogonal decomposition; low rise structures; full scale experiments; ventilation.

1. Introduction

The technique of proper orthogonal decomposition of surface pressures (first described by Armitt 1968) assumes that the fluctuating surface pressure coefficient on a structure can be given by the following series.

$$C_p' = P_1 T_1 + P_2 T_2 + P_3 T_3 + \cdots\cdots \tag{1}$$

Here P_i are functions of spatial position and T_i are functions of time i.e., the pressure coefficient can be expressed as a series of spatial and temporal functions. Now by making the assumptions that

a) the functions P_i are orthogonal (i.e., the scalar product of any pair of these functions is zero), and
b) the functions T_i are uncorrelated in time,

then it is possible to show that the functions P_i are the eigenvectors of the pressure coefficient covariance matrix, and the mean square values of the functions T_i are the eigenvalues of that matrix. In addition it can be shown that the sum of the eigenvalues is equal to the integral of the mean square fluctuating pressure coefficient over the surface and that the spectrum and r.m.s. of the fluctuating pressure coefficients can be given by

$$S_{cpcp} = P_1^2 S_{T1} + P_2^2 S_{T2} + P_3^2 S_{T3} + \cdots\cdots \tag{2}$$

† Professor of Environmental Fluid Mechanics

and

$$\sigma_{cp}^2 = P_1^2\overline{T}_1^2 + P_2^2\overline{T}_2^2 + P_3^2\overline{T}_3^2 + \cdots\cdots \quad (3)$$

where S_{Ti} is the spectrum of T_i and the overbar indicates time averaging. The latter expressions will be seen to be of some interest in what follows.

The main utility of this method is that it is found in practice that only the first few modes contain significant energy, and thus in principle the entire fluctuating flow field over a structure can be represented by a relatively short series of spatial and temporal functions. The application of this to the calculation of the extreme wind pressures on structures is outlined by Holmes (1990).

This technique is essentially a variant of Karhunen - Loeve decomposition and a type of Principal Component Analysis (Tamura *et al*. 1999). The modes that are identified effectively represent the orthogonal principal axes in N component phase space that best represent the pressure fluctuations over the surface.

Now within the literature there is a degree of controversy as to whether or not the modes identified through the application of this technique can be associated with specific physical causes. Up till recently there has been the fairly unanimous agreement that for low rise structures, the first mode is directly associated with longitudinal quasi-steady fluctuations, based largely on the qualitative similarity between the mean pressure distribution and the shape of the first eigenvector - see Best and Holmes (1983), Letchford and Mehta (1993) and Prevezer *et al*. (1997). For high rise structures with strong vortex shedding Kareem and Cermak (1984), Kikuchi *et al*. (1997) and Tamura *et al*. (1999) associate the strongly asymmetric first mode with vortex shedding, which is consistent with the more fundamental work around prismatic cylinders reported by Lee (1975). Whilst the first mode is thus able to be consistently identified with a physical mechanism, there is greater uncertainty about the higher modes, with different authors assigning different physical causes to the modes that they observed - lateral and vertical turbulence, wake vortex shedding, locally separated flow etc. Nonetheless there was general agreement that such relations did exist. However Holmes *et al*. (1997) argued that the mode shapes they observed were largely determined by the constraints of orthogonality, and identifications with physical causes are likely to be fictitious. This was based on two studies. The first was a comparison of the mode shapes over a pitched roof building with different opening configurations and sampling regions. It was shown that the eigenvectors were dependent upon the configuration and sampling region and this was said to be because of the constraints of orthogonality. The second investigation was based on “theoretical” mode shapes that were very similar to the measured shapes along the span of a pitched roof building and it was argued that since this equation had no physical basis, neither had the modes. Clearly there is a level of disagreement over whether or not it is sensible to identify POD modes with physical mechanisms. This paper addresses this issue in some detail through a detailed analysis of some full scale experimental data and through a study of a theoretical solution to a specific problem. This is followed by a discussion of other issues where this technique might be useful - in particular the ventilation of multi-opening enclosure and the correlation between internal and external pressures in such enclosures.

2. Can the modes be associated with physical causes?

2.1. Basic considerations

Firstly consider the assumptions of orthogonality and non-correlation outlined above. These

effectively assume that the modes are both spatially and temporally independent. If the modes actually represent distinct physical phenomena that together produce the fluctuating surface pressures then this implies that these phenomena should also be spatially and temporally independent. Now consider a typical structure in the natural wind. Surface pressure fluctuations may plausibly be caused in a number of ways - by the different components of turbulence in the upstream flow, by large scale wake unsteadiness, by smaller scale unsteadiness in separated flow regions etc. To a first approximation one would expect these physical mechanisms to be independent and uncorrelated, but not completely so. For example separated shear layers may exhibit an inherent unsteadiness, but this will almost certainly be modified by oncoming turbulence etc. Thus one might expect that the most energetic (lower) modes of a proper orthogonal decomposition of the pressure field would each reflect to some degree a specific physical mechanism, but any particular mode might also contain some component due to other physical causes. The less energetic (higher) modes one would expect to each be influenced by a number of physical causes. In other words it does not seem unreasonable to assume that the lower three or four modes are related to distinct physical phenomena, but some degree of interaction should be expected both in these modes, and in the higher modes.

Further the number of modes identified in a particular case will be equal to the number of experimental points. Whilst for some highly detailed wind tunnel tests this might be in the region of a few hundred points, for most wind tunnel tests and for all full scale measurements this figure will be much smaller - probably of the order of 10 to 50. It would thus be expected that the highest modes will in some way be affected by the truncation of what must be, in the limit, an infinite series. Further it may also be expected that small errors in experimental data may significantly affect these higher less energetic modes in particular.

To test these ideas we firstly consider (in 2.2 and 2.3) three sets of full scale experimental results, and attempt to analyse the lower modes in each case in terms of identified physical mechanisms. We then in 2.4, through a consideration of a theoretical solution to a specific covariance set, consider the effect of truncating the number of modes, and of random errors.

2.2. Experimental datasets

In what follows we consider the results of an analysis of three full scale datasets obtained by staff at Silsoe Research Institute - a two dimensional wall, a large cube and a pitched roof agricultural building.

2.2.1. The wall

The details of the experimental wall are given in Robertson *et al*. (1997). It was built in order to obtain pressure coefficients for use in wind loading design codes, and previous data analysis has been directed towards that end. It was built such that its length could be varied, return corners could be fitted etc., and consisted of a number of 2 m square panels. The data that will be used in this investigation is for a 9 panel wall, 18 m long and 2 m high, with a mean wind direction more or less normal to its long axis. Details of the experimental conditions are given in Table 1. Results will be presented for pressure measurements at the centre of each panel. Tappings 1 to 9 were on the windward side of the wall and tappings 10 to 18 were the corresponding panels on the leeward side of the wall (Fig. 1a). These measurements were sampled at a rate of 5 Hz, and pressure coefficients were formed using the instantaneous pressures and the mean wind speed.

Table 1 Experimental conditions for full scale data

	Wall	Cube	Building
Mean wind angle to windward face (degrees)	-1.2	-5.5	3.2
Reference height (m)	2	6.0	5.3
Mean velocity (m/s)	9.68	11.60	9.05
Longitudinal turbulence intensity	0.283	0.230	0.232
Lateral turbulence intensity	0.217	0.170	0.182
Vertical turbulence intensity	0.092	0.097	0.078

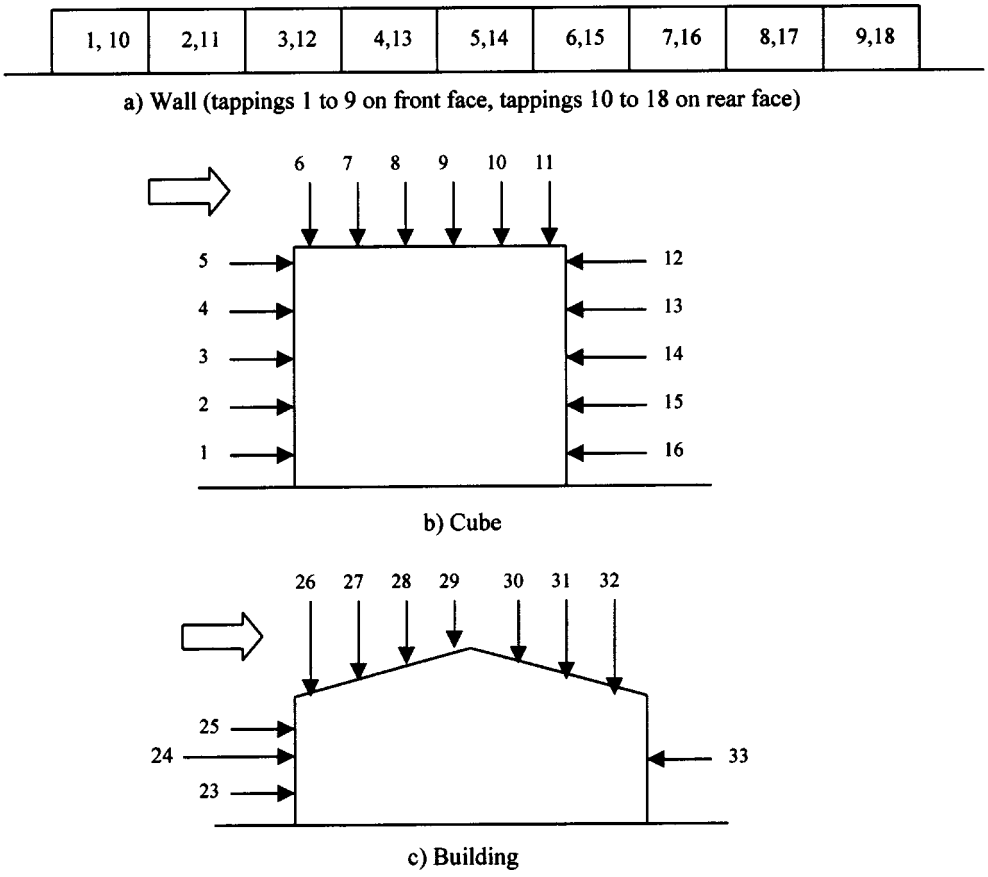

Fig. 1 Sketch of pressure tap locations

2.2.2. The cube

The experimental cube has sides of 6 m, and is able to rotate around its vertical axis, and also to tilt to some degree. Brief details of this facility are given in Hoxey *et al.* (1999). The data used in this paper were obtained with the wind normal to one face of the cube. Again details are given in Table 1. Pressures were measured at tappings on the centre line of the cube, taps 1 to 5 on the cube front face, taps 6 to 11 on the cube roof, and taps 12 to 16 on the leeward face (Fig. 1b). Pressures

were again sampled at 5 Hz, and pressure coefficients formed as above. Flow visualisation indicated a separation bubble over the roof of the cube, with a reattachment towards the leeward edge.

2.2.3. The building

The building is a pitched roof low rise agricultural structure, 4 m high to the eaves, 24 m wide and 12 m deep with a roof slope of 10 degrees (Hoxey *et al*. 1995, Richardson *et al*. 1995). It had two basic configurations - with either sharp or curved eaves. In what follows we will consider results for the centreline of the building with the wind normal to the long face, for the sharp eaves case only. In this case flow visualisation showed that the flow separated over the windward eave and reattached halfway up the windward roof. The flow then remained attached over the ridge before separating half way down the leeward face. The pressure was measured at 11 taps around the centreline, numbered from 23 to 33. Taps 23 to 25 are on the windward wall, taps 26 to 29 on the windward roof, taps 30 to 32 on the leeward roof and tap 33 on the leeward wall (Fig. 1c). It is important to note that on the windward roof taps 26 and 27 are within the separation region on the windward roof, tap 28 somewhere near the point of reattachment, and tap 29 in an attached flow region. The experimental results that will be considered were obtained for the wind conditions given in Table 1. A 20 Hz sampling rate was used to obtain this data.

2.3. POD analysis of experimental data

A POD analysis gives 18 modes for the wall data, 16 modes for the cube data and 11 modes for the wall data. As has been found by other investigators the eigenvalues for the lower modes are significantly greater than those for the higher modes. Fig. 2 shows the cumulative energy within the modes (as given by the sum of the eigenvalues up to that mode). It can be seen that 90% of the total energy is given within the first five or six modes. Fig. 3 shows the eigenvectors for the wall data (separately for the front and rear faces), Fig. 4 shows the eigenvectors for the cube data and Fig. 5 shows the data for the building. Fig. 6 presents the mode spectra for the lower two modes for each case, expressed in terms of an admittance with the longitudinal velocity spectrum $(S_{TiTi}/s_{uu})(\sigma_{uu}^2/\overline{T}_{i2})$. Before proceeding to discuss these results it is however worthwhile to consider the results of Fig. 7 which presents data for modes 4 and 5 for the cube from nominally similar datasets (subsets of that

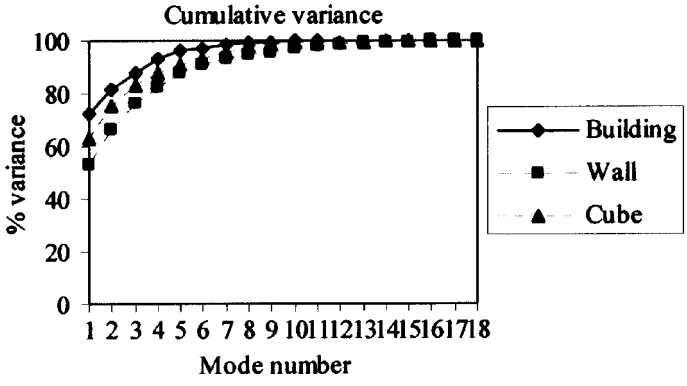

Fig. 2 Cumulative percentage energy by mode

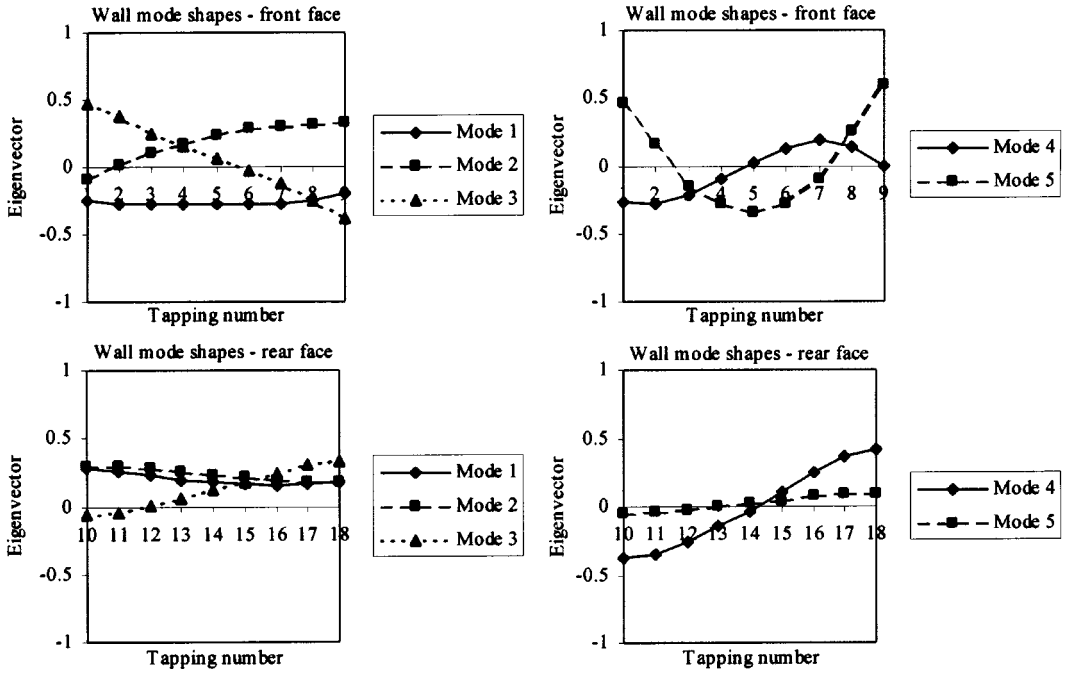

Fig. 3 Mode shapes for wall

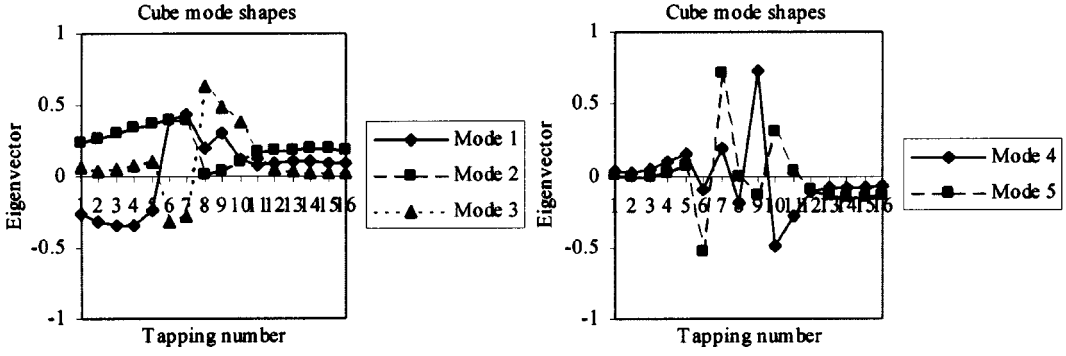

Fig. 4 Mode shapes for cube

used to give the results of Fig. 4), with slightly different mean wind speeds and directions. Whilst for these datasets modes 1 to 3 were in good agreement, it can be seen that the modes shown vary significantly. Tamura *et al*. (1999) show that for flows with a "singular" condition (taken as meaning an intermittent switching between different flow patterns) then different sets of data for nominally identical conditions can give different eigenvector distributions. Whilst the flows studied in this paper are likely to be in general stable, it may be that the less energetic modes could be affected in this way, which may explain the results of Fig. 7. In any case, because of this discrepency, no attempt will be made to assign physical meanings to modes 4 and higher in any of the datasets, and the discussion below will focus on modes 1 to 3.

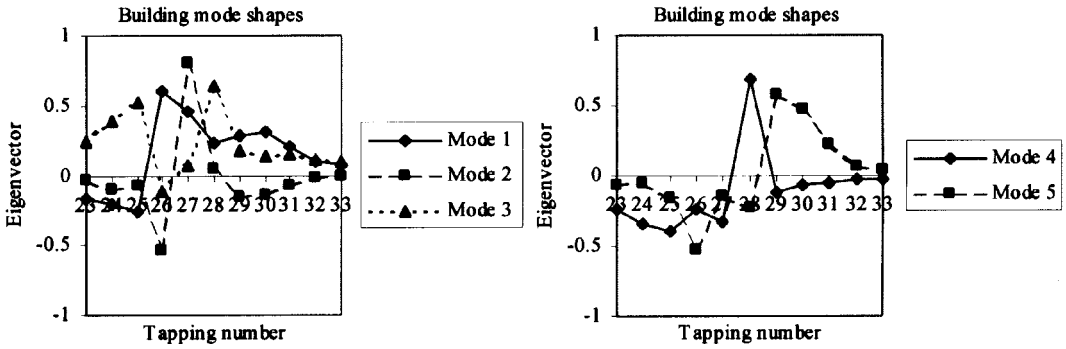

Fig. 5 Mode shapes for building

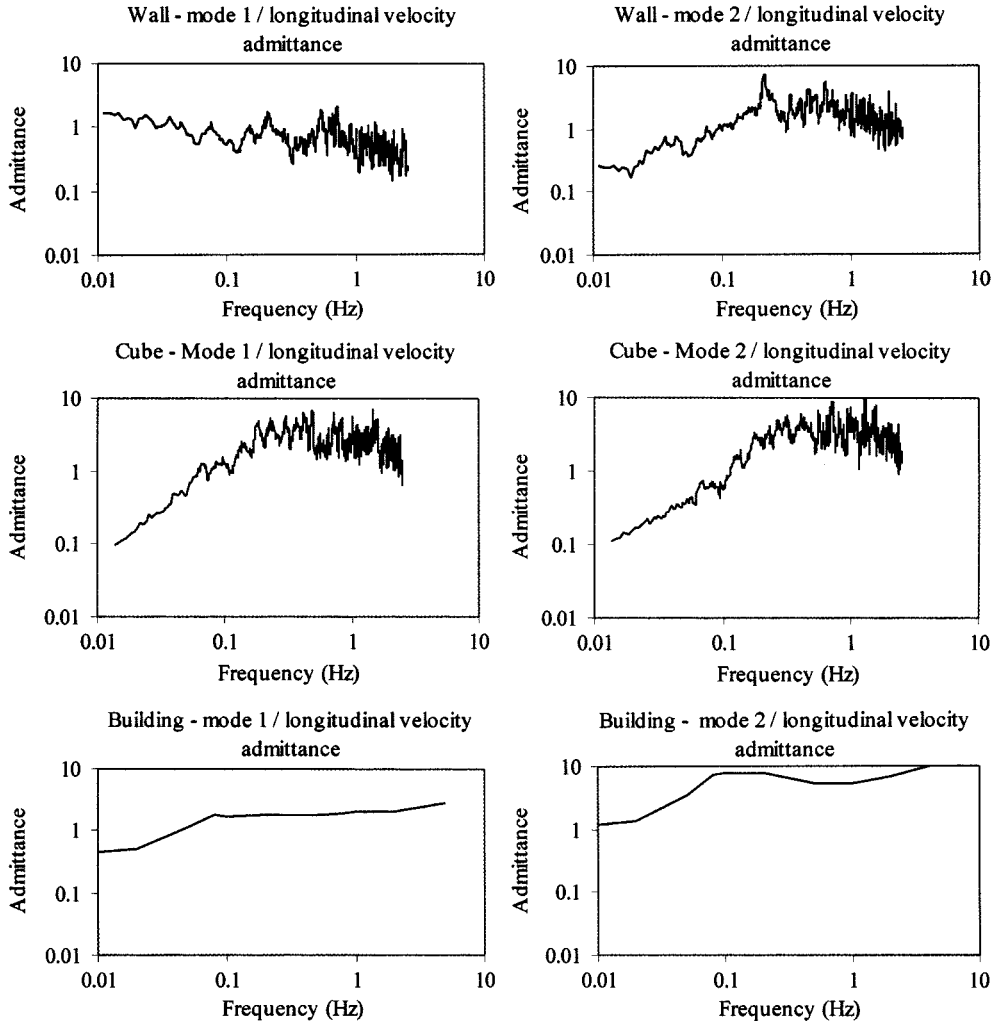

Fig. 6 Longitudinal velocity admittances for wall, cube and building modes 1 and 2

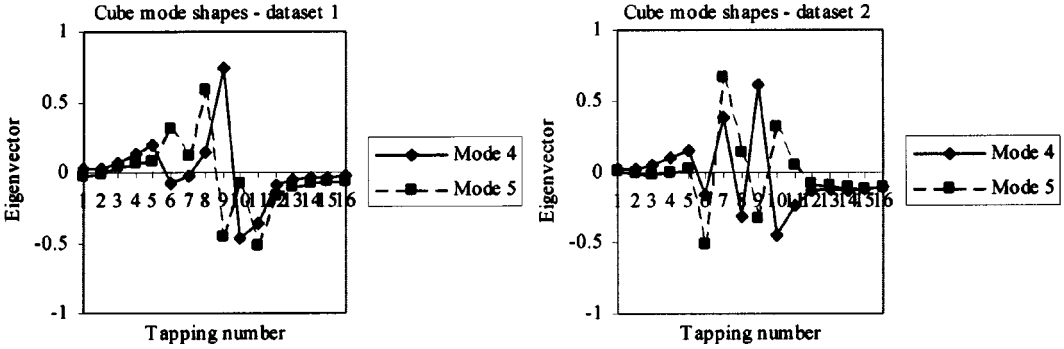

Fig. 7 Modes 4 and 5 for cube from nominally similar datasets

Now for the structures considered here one can postulate that there are a number of physical phenomena that are responsible for the fluctuating pressure field. These are

a) quasi-steady fluctuations due to the longitudinal, lateral and vertical oncoming turbulence;
b) fluctuations due to a large scale wake unsteadiness;
c) fluctuations due to unsteadiness in the separation regions.

Let us first consider the postulated quasi-steady fluctuations. If non linear effects are ignored and correlations between the different components of turbulence assumed small, then at any point on a structure the variance of the fluctuations caused by such mechanisms should have the form

$$\sigma_{cpcp}^2 = 4\overline{C}_p^2\left(\frac{\sigma_{uu}}{\overline{u}}\right)^2 + \left(\frac{d\overline{C}_p}{d\theta}\right)^2\left(\frac{\sigma_{vv}}{\overline{u}}\right)^2 + \left(\frac{d\overline{C}_p}{d\phi}\right)^2\left(\frac{\sigma_{ww}}{\overline{u}}\right)^2 \tag{4}$$

Here $\overline{C}_p$ is the mean pressure coefficient, $\sigma_{uu}/\overline{u}$, $\sigma_{vv}/\overline{u}$ and $\sigma_{ww}/\overline{u}$ are the longitudinal, lateral and vertical components of turbulence, θ is the instantaneous lateral flow direction and ϕ is the instantaneous vertical flow direction. The three terms in the above equation represent longitudinal, lateral and vertical quasi-steady fluctuations respectively. Further terms could be added to describe second order effects, but for the sake of simplicity they will not be considered in the analysis presented here. For the wall data all the terms in Eq. (4) can be expected to be non-zero. The first term can be calculated from the mean pressure coefficients, and the second term can be found using the value of the lateral pressure derivative $d\overline{C}_p/d\theta$ obtained from experiments for different wind directions. It is not possible to specify the third term since that involves the vertical pressure derivative $d\overline{C}_p/d\phi$ which was not measurable. For the cube data, the first term can again be calculated from the mean pressure coefficient. Because we are dealing with centreline data the second term can be expected to be zero, because the lateral pressure gradient will be zero from considerations of symmetry. Because the cube was able to be tilted, it was possible to derive the vertical pressure coefficient gradients for this case, and thus the third term could be calculated. For the building case, the first term could again be obtained from the mean values of the pressure coefficients. Again as centreline data is being used, $d\overline{C}_p/d\theta$ must again be zero because of symmetry. As it was not possible to measure vertical derivatives in this case, the third term could again not be calculated.

Now if for any of the cases under consideration a particular mode i is due primarily to longitudinal quasi-steady effects then one would expect firstly that the modal spectra would have a

shape similar to the longitudinal turbulence spectrum of the upstream velocity (or alternatively the modal admittances will be close to unity across the frequency range), and that, by a comparison of Eqs. (3) and (4)

$$P_i^2 \overline{T}_i^2 = 4\overline{C}_p^2 \left(\frac{\sigma_{uu}}{\bar{u}} \right)^2 \tag{5}$$

In the past several authors have argued that the first mode should represent longitudinal quasi-steady effects. Now it can be seen from the admittances of Fig. 6 that for the first mode the wall data is close to unity, but this is not particularly the case for the cube and the building. The difference may lie in the height of the reference anemometer. For the wall experiments this height was much closer to the height of the stagnation streamline (which is some sort of representative streamline for the structure). At the height of the stagnation streamline for the cube and building cases there can be expected to be a significant shift in energy to higher frequencies than for the streamline at the reference velocity position. This is consistent with the admittances in Fig. 6.

Fig. 8 shows a plot of the measured eigenvectors for mode 1 for each case and those predicted assuming longitudinal quasi-steady fluctuations. It can be seen that in general there is good agreement, although there are some discrepancies particularly on the rear of the wall and in the separation regions on the roof of the cube and the building. Nonetheless these Figures strongly suggest that for each set of experimental data mode 1 is associated with longitudinal quasi-steady effects to a great extent. It is of particular interest to note the importance of these quasi-steady fluctuations at the roof leading edge on the cube and building (taps 6 and 26 respectively), at the

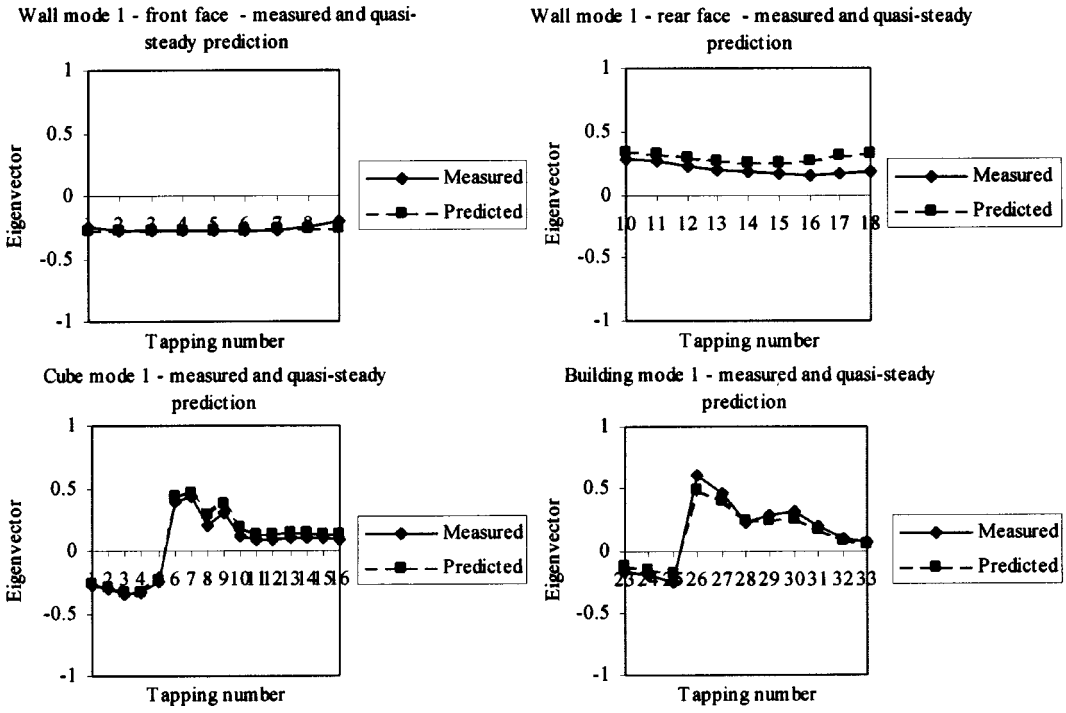

Fig. 8 Measured and longitudinal quasi-steady predictions for wall, cube and building mode 1

front of the separation region. This might perhaps be caused by the oncoming turbulence causing a flapping of the separated shear layer near this point.

Now consider lateral quasi-steady fluctuations. If a mode i represents these fluctuations than one would expect its spectrum to be similar in shape to the lateral turbulence spectrum, and by a comparison of Eqs. (3) and (4)

$$P_i^2 \bar{T}_i^2 = \left(\frac{d\bar{C}_p}{d\theta}\right)^2 \left(\frac{\sigma_{vv}}{\bar{u}}\right)^2 \tag{6}$$

The wall data is the only dataset that should show this effect. The mode 2 admittance for the wall rises sharply with frequency when formed with both the longitudinal velocity spectrum (Fig. 5) and the lateral velocity spectrum (not shown). Fig. 9 shows the same admittances for the wall mode 3 data. Both are flat and near to unity, and thus mode 3 could be a potential candidate for association with lateral quasi-steady fluctuations. Fig. 10 shows a comparison of the predicted and calculated mode shapes for this mode. The two sets of results can be seen to be similar in form, although the precise values are somewhat different. These results suggest that this mode may be to some degree associated with lateral quasi-steady fluctuations.

Consider now vertical quasi-steady fluctuations. Again if a mode i represents these fluctuations than one would expect its spectrum to be similar in shape to the vertical turbulence spectrum, and

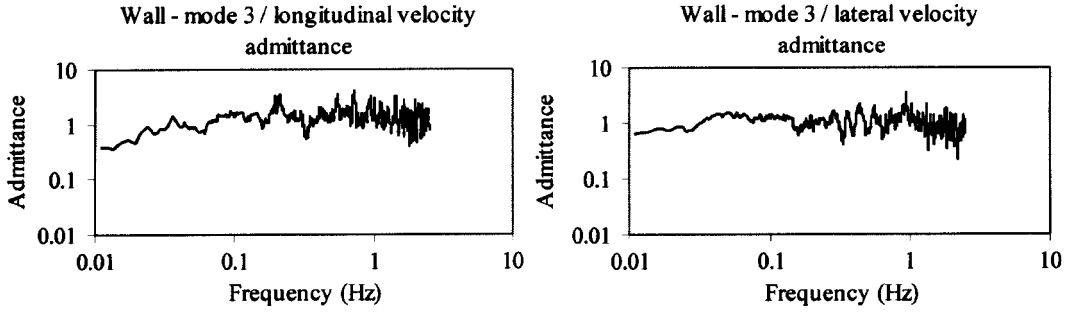

Fig. 9 Longitudinal and lateral velocity admittances for wall mode 3

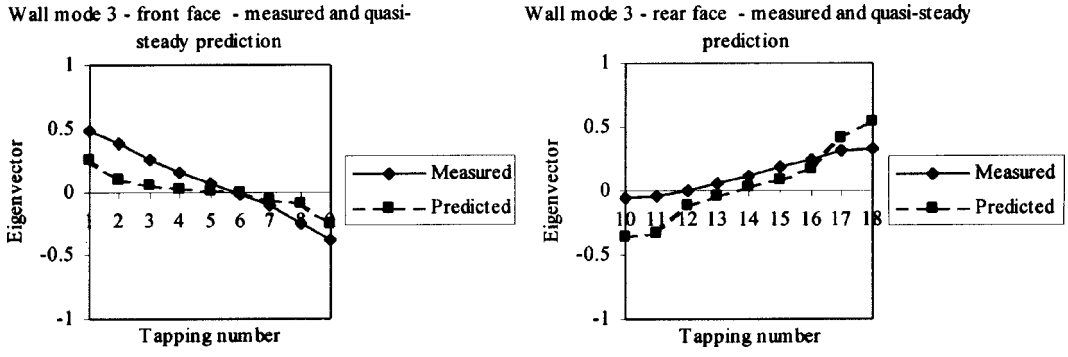

Fig. 10 Measured and lateral quasi-steady predictions for wall mode 3

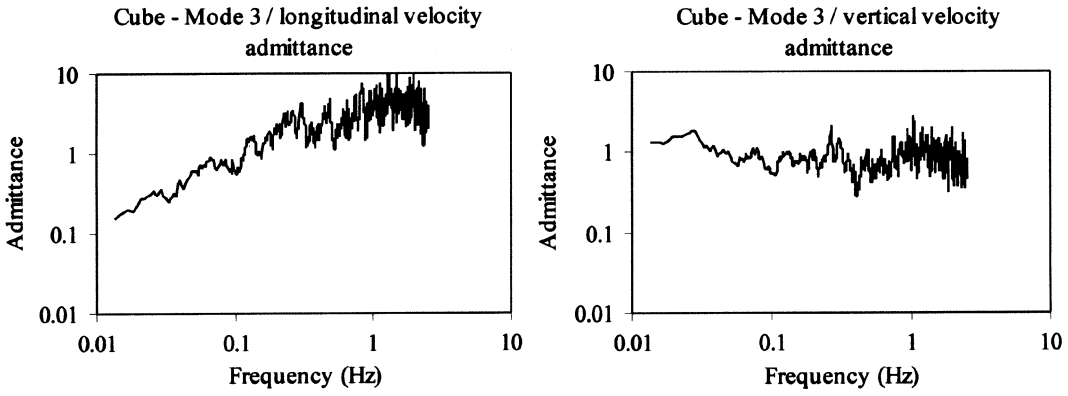

Fig. 11 Longitudinal and vertical velocity admittances for cube mode 3

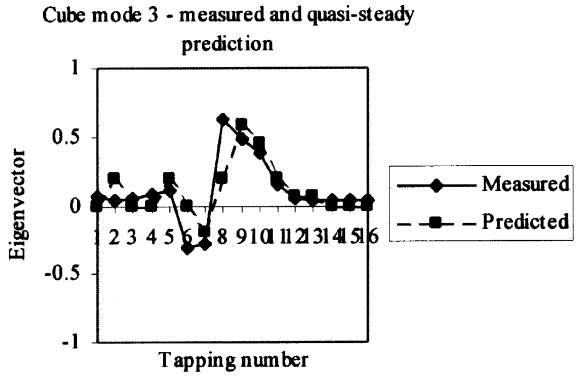

Fig. 12 Measured and vertical quasi-steady prediction for cube mode 3

by a comparison of Eqs. (3) and (4)

$$P_i^2 \overline{T}_i^2 = \left(\frac{d\overline{C}_p}{d\phi}\right)^2 \left(\frac{\sigma_{ww}}{\bar{u}}\right)^2 \tag{7}$$

Because it was possible to tilt the cube and obtain vertical pressure coefficient derivatives, it should be possible to identify any such mode from this data. For this data the mode 2 admittances again increased very significantly with frequency when formed with both longitudinal velocity spectrum (Fig. 6) and the vertical velocity spectrum (not shown). The third mode however, whilst increasing with frequency when formed with the longitudinal velocity spectrum, was relatively flat and close to unity when formed with the vertical velocity spectrum (Fig. 11) and is thus a candidate for association with vertical quasi-steady fluctuations. The predicted and measured eigenvectors are shown in Fig. 12. The agreement can be seen to be relatively good, and suggests that for the cube data the third mode is associated with vertical quasi-steady effects. It is of interest that this mode is particularly significant at taps 8 and 9 (which are near the reattachment point). If, by analogy, mode 3 for the building is also associated with vertical quasi-steady effects the large peak in this mode at tapping 28, which is near the reattachment point, is similar in nature, and suggests a major role in vertical quasi-steady fluctuations around roof reattachment.

Now consider fluctuations due to large scale wake unsteadiness. If a particular mode represented

such fluctuations one would expect the eigenvectors for these modes to peak in the regions of such separated flow (i.e., in the lee of the wall, cube and building) and for the spectra (and thus the admittances to show a peak at a value of frequency of around (reference velocity / representative building dimension). Assuming a representative dimension for the wall of 2 m and for the cube and building of 6 m, the frequencies should thus be around 5 Hz, 2 Hz and 2 Hz for the three structures. An examination of Fig. 3 to 5 for the eigenvectors reveal no modes that meet the first of these criteria. The admittances for modes 4 and 5 (not shown) on all three structures do however show significant energy in the range above 1 Hz. However it was argued above that modes 4 and 5 can show considerable variation between nominally similar datasets (section 2.3), and it would be unwise to assign precise physical meanings to them. Thus it does not appear that there is conclusive evidence that any of the lower modes are associated with large scale wake unsteadiness, at least for the cases considered here.

Finally consider fluctuations due to unsteadiness in locally separated flow regions. The first test of whether or not a particular mode represents these fluctuations should be a peak in the eigenvector within these regions and little energy elsewhere i.e., in the separated flow regions on the roofs of the cube and building. Modes 4 and 5 for the cube and modes 2 and 4 for the building fulfill this criterion. For the reasons above it would be unwise to consider modes 4 and 5 as having precise physical causes however. Secondly Cherry *et al.* (1984), in their fundamental investigation of separation bubbles, identified a peak in the surface pressure spectra from downstream of about 60% of the separation bubble length with a frequency of (0.7 $\times$ free stream velocity / separation length). For the case of the separation bubble on the windward roof of the building (with an assumed separation length of about 3 m), this corresponds to a peak in the spectrum at about 2 Hz. There is a flat peak in the admittance for mode 2 at about this frequency (Fig. 6). The identification of mode 2 with fluctuations in the separation region is further confirmed by the curved eaves results (given in Prevezer 1998) where a separation bubble does not exist. No mode similar to mode 2 exists in this data.

Thus in summary it would seem that there is fairly strong evidence that for the cases under consideration, the first mode represents mainly longitudinal quasi-steady fluctuations. For the building mode 2 represents a fluctuation due to the separation bubble above the roof of the structure. For the wall mode 3 fluctuations appear to be largely due to lateral quasi-steady wind fluctuations, whilst for the cube, and quite possibly the building, mode 3 represents vertical quasi-steady fluctuations. This still leaves the question as to what, if anything, is represented by mode 2 on the wall and the cube and the higher modes in each case. The higher modes will be discussed below. With regard to mode 2 on the wall and cube, it is possible that these modes might in some way reflect the effect of streamline distortion on the quasi-steady fluctuations (see Hoxey *et al*. 1999), but at this stage this is merely conjecture.

This conclusion is less pessimistic than that reached by Holmes *et al.* (1997). They argued that the identification of mode shapes with physical mechanisms was likely to be fictitious. As mentioned in section 1 this conclusion was based on two studies. The first was a comparison of the mode shapes over a pitched roof building with different opening configurations and sampling regions. It was shown that the eigenvectors were dependent upon the configuration and sampling region. This was said to be because of the constraints of orthogonality. There is however another possibility - that this difference is simply due to different physical mechanisms being present for different opening configurations, and these modes being identified only when the sampling area is significantly affected by these mechanisms. A close inspection of the results of Holmes *et al.* shows that similar mode shapes exist in different configurations, although the mode order is different. Indeed the same effect

can be found in the present data - if for example only the windward pressure tappings on the wall were used in a POD analysis, a number of modes were eliminated that probably primarily reflect leeside flow mechanisms. The second investigation described by Holmes *et al*. will be considered further in the next section.

At this point it is also appropriate to mention the work of Tamura *et al*. (1995). They attempted to determine whether or not modes were associated with physical causes, by finding correlation coefficients between the mode time series and the measured upstream velocity component. This is a somewhat cruder approach than that adopted here, but was directed towards the same ends. For their low rise building, which was instrumented across its surface with up to 500 pressure tappings. They were only able to find significant correlation between mode 1 and the longitudinal velocity component, and between mode 2 and the lateral velocity component. Even for these the correlation coefficients did not exceed 0.5 for the first mode and 0.35 for the second mode. This lack of good correlation probably reflects the facts that the reference point was someway upstream of the model (and thus only low frequency components could be expected to be correlated) and also that there is not a precise one to one relationship between individual modes and physical mechanisms.

2.4. Theoretical considerations

Holmes *et al*. (1997) show that if the pressure coefficient covariances can be expressed in the form

$$C = \sigma^2 e^{-k|x|/a} \tag{8}$$

where σ^2 is the integrated variance of the fluctuating pressure coefficients, $|x|$ is the magnitude of the distance between any two points, $\pm a$ is the range of the calculation and k is a constant, then the eigenvalues are given by

$$\lambda = \frac{2ka\sigma^2}{y^2 + k^2} \tag{9}$$

For odd modes the function y and the eigenvectors ϕ are given by

$$y = \frac{k}{\tan y} \qquad \phi = \frac{(2y/a)^{0.5}\cos(yx/a)}{(2y + \sin 2y)^{0.5}} \tag{10}$$

and for even modes they are given by

$$y = -k\tan y \qquad \phi = \frac{(2y/a)^{0.5}\sin(yx/a)}{(2y - \sin 2y)^{0.5}} \tag{11}$$

Holmes *et al*. show that the form of Eq. (8) adequately describes the covariance distribution over a spanwise section on the roof of the low rise building that they were investigating, although there is no reason why it should apply in other situations. They went on to argue that since this equation had no physical basis, neither had the modes that they observed experimentally. It is however possible that this agreement was simply because Eq. (8) was a reasonable empirical fit to the measured covariances which themselves were the results of specific flow mechanisms. In any case these equations allow the calculation of an infinite series of eigenvalues and eigenvectors. To check what the effect is of reducing the number of sampling points, and thus truncating the infinite series, covariances were generated for three cases as follows

a) using Eq. (8) but for 20 equally spaced points over the range;
b) as in (a) but for 10 equally spaced points over the range;
c) as in (b) but with a random error of between 0 and 0.03 applied to the generated covariances.

The eigenvalues and eigenvectors were then calculated for the resulting covariance matrices. In what follows the calculated eigenvalues will be normalised with $a\sigma^2$, the eigenvectors with $(1/\sigma a)^{0.5}$

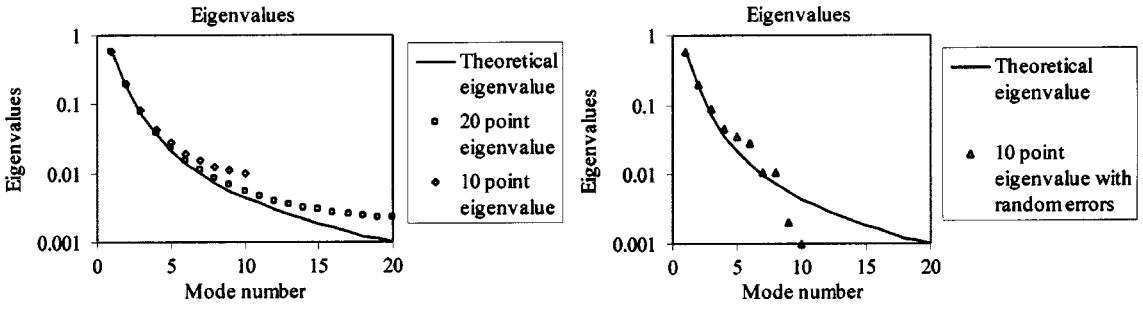

Fig. 13 Effect of discretisation and random errors on theoretical eigenvalues

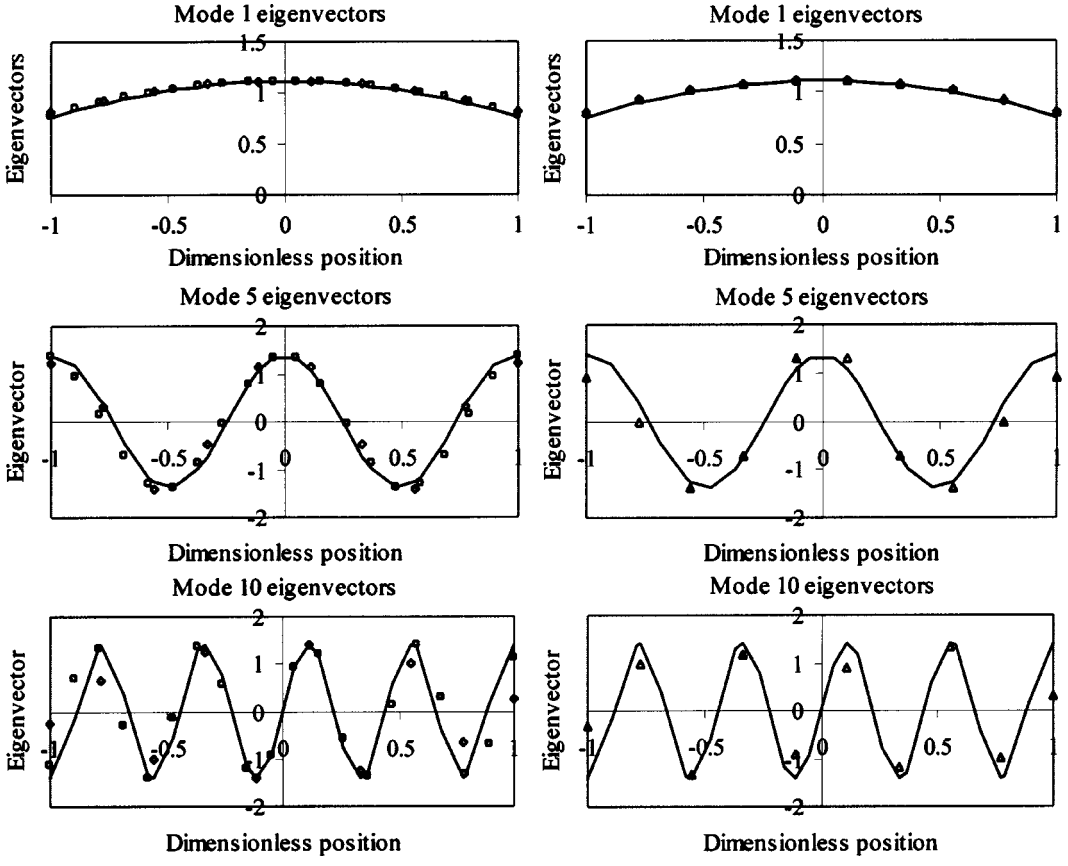

Fig. 14 Effect of discretisation and random errors on theoretical eigenvectors (for key see Fig. 13)

and distances with *a*. The value of *k* is taken as 0.888 as in Holmes *et al*. It can be seen from Fig. 13 that the eigenevalues are in agreement with the theoretical values for the lower modes, but begin to deviate considerably from theory for the higher modes. As a rule of thumb it would appear that the eigenvalues begin to show significant errors for modes N/2 and above, where N is the total number of modes in each case. The effect of a random error is also significant in this range. The eigenvectors themselves (Fig. 14) seem to be relatively insensitive to series truncation except that for case (b) above the number of points across the range is too small to fully represent the true "sinusoidal" nature of the eigenvector for mode 10. In general the effect of the random errors is small, although there is considerable scatter for the mode 10 results.

It can thus be concluded that the higher modes are likely to be significantly affected by the effect of spatial discretisation and experimental error, and that it would be unwise to assign any physical meaning to these modes. This does not of course mean that these modes cannot be used to represent the original fluctuating pressure dataset.

3. Other applications of proper orthogonal decomposition

Holmes (1990) has shown that the technique of proper orthogonal decomposition is in principle useful in enabling the extreme values of loading to be calculated simply from the extreme values of the lower, most energetic modes. It is the purpose of this section to briefly point out a few other applications of the technique that are potentially useful, and also, if one accepts that the modes do represent physical phenomena to some degree, offer an insight into the nature of the flow around structures.

Firstly we consider the use of POD in describing the ventilation of multi-opening enclosures. This has been briefly considered by the author in Baker (1998). In that paper he showed, through a consideration of a linearised equation of ventilation rate through such an enclosure (following Haghighat *et al*. 1991) that the spectrum of the ventilation rate could be given by

$$S_{QQ} = \frac{(\omega\rho V u^2/2k)^2(\prod_1^2 S_{T1} + \prod_2^2 S_{T2}\cdots\cdots)}{\left(\left(1-\frac{\omega^2}{\omega_n^2}\right)^2 + \left(\frac{2c\omega}{\omega_n}\right)^2\right)} \tag{12}$$

where ω is an angular frequency, ω_n is the natural frequency of the system (= $(ABN/\rho L)^{0.5}$) and c is the damping of the system (= $k/2(\rho LABN)^{0.5}$); ρ is the density of air, V is the volume of the enclosure, u is a reference velocity, k is a coefficient of linearisation, A is the orifice area, L is the effective opening length (calculated from (actual opening length + 0.89 (opening area)$^{0.5}$)) and N is the number of orifices; $B = \gamma P_R/V$ where γ is the ratio of specific heat and P_R is a reference pressure; $\prod_i = \sum_j P_i(x_j)/N$ where subscript i indicates the mode and subscript j the position of the orifices on the surface

A hypothetical calculation was carried out for ventilation into the Silsoe building with openings at the positions of tappings 29 and 30 (on the windward and leeward sides of the ridge respectively), thus rather artificially simulating a ridge ventilator. The values of the assumed parameters are shown in Table 2 below. These were such that the natural frequency was 1.48 Hz and the damping ratio was 0.189. In this simulation the ventilation spectra were calculated by mode using Eq. (12) and the results are shown in Fig. 15. The spectra can be seen to peak at the natural frequency of the system

Table 2 Parameters assumed for ventilation calculation

A (m^2)	ρ (kg/m^3)	Opening length (m)	L (m)	V (m^3)	k	u (m/s)	N	γ	P_R (Pa)
0.5	1.25	0.05	0.675	1900	3	5	2	1.4	100000

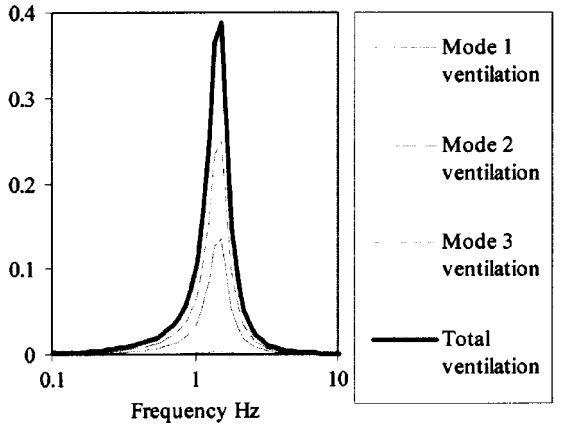

Fig. 15 Modal and total ventilation spectra for hypothetical building ventilation

as would be expected. It can further be seen that in this case the ventilation is dominated by the third mode, identified above with vertical quasi-steady effects, which in view of the importance of this mode on the building roof is not unexpected. The next most important ventilation mode is mode 1, due to longitudinal quasi-steady effects. The unsteady ventilation rates for each mode can then be found from an integration of the spectra. For this case, in terms of air changes / hour (ach), it was found that the mean ventilation component was 0.335 ach. This Figure was calculated by assuming orifice flow through the openings driven by the external pressure difference, with a discharge coefficient of 0.61. The unsteady ventilation rates for each mode could be calculated from the simple formula

$$(\sigma_i^2)^{0.5}(\sqrt{2}/\pi)(3600/V)$$

where σ_i^2 is the variance of the modal variation calculated from integrating beneath the ventilation spectrum. The mode 1, 2 and 3 ventilation rates were, respectively 0.236, 0.041 and 0.321 ach. Thus the unsteady ventilation can be seen to be the main component of ventilation in this case. Whilst this is a purely hypothetical example it can be seen that the use of the technique of POD allows both a relatively simple calculation to be made, and also allows a degree of physical insight into the phenomenon.

Next we consider the use of POD in investigating the relationship between the internal and external pressure fluctuations within a building, and thus to consider the loading on the cladding of a structure with a single skin. From the ventilation analysis outlined above the spectrum of internal pressure within a structure can be expressed as

$$S_{cp} = \frac{\left(\prod_1^2 S_{T1} + \prod_2^2 S_{T2} \cdots\cdots\right)}{\left(\left(1-\frac{\omega^2}{\omega_n^2}\right)^2 + \left(\frac{2c\omega}{\omega_n}\right)^2\right)} \tag{13}$$

From a consideration of the external pressure at the cladding point (denoted by c) and the internal pressure the following equation can be derived for the spectrum of the net pressure coefficient on the cladding element

$$S_{cpc} = \sum_{i=1}^{i=N} \frac{\left(\left(1-\frac{\omega^2}{\omega_n^2}\right)^2 (P_{ic} - \prod_i)^2 + \left(\frac{2c\omega}{\omega_n}\right)^2 P_{ic}^2\right) S_{Ti}}{\left(\left(1-\frac{\omega^2}{\omega^2}\right)^2 + \left(\frac{2c\omega}{\omega_n}\right)^2\right)} \tag{14}$$

Thus again it can be seen that the use of POD allows a reasonably straightforward description of the net cladding pressure to be obtained, and the use of only the first few terms will allow the spectrum to be suitably specified. The external, internal and cladding pressure spectra from such a procedure are shown in Fig. 16 for the Silsoe building ventilated as described above, for an element of cladding at the location of tap 26, near the windward leading edge and thus within the separated flow region. It can be seen that a peak in the internal and net cladding spectrum is predicted corresponding to the natural frequency of the enclosure. From such spectra it is possible, through a routine extreme value analysis, to find the extreme values of the cladding pressure that allows for the correlation of internal and external pressures. Table 3 shows the results of such a calculation for this case. It can be seen that such a calculation allows for the actual minimum cladding pressure to be calculated, rather than the more conservative value obtained from the mean internal pressure and the minimum external pressure. Whilst the results are very specific to the hypothetical situation

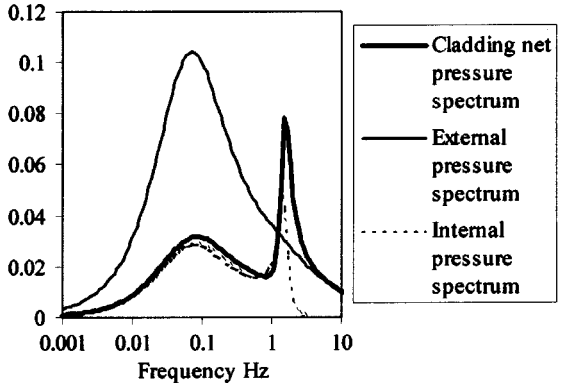

Fig. 16 External, internal and cladding spectra for hypothetical building ventilation

Table 3 Calculated cladding pressure coefficients for Silsoe Building tapping 26 (1s averages)

Parameter	Value
Mean external coefficient	-1.389
Mean internal coefficient	-0.696
Mean cladding coefficient	-0.693
Min external coefficient	-2.526
Min internal coefficient	-1.295
Min cladding coefficient	-1.326

being considered, this method can be seen to give a rational way of allowing for the correlation between internal and external pressure coefficients when calculating cladding loads.

4. Conclusions

The first part of this paper addressed the question as to whether or not the modes identified by a POD analysis can be associated with physical flow phenomena. On the basis of an analysis of experimental data and an analytical / numerical investigation it was concluded that

a) The lower (more energetic) modes are likely to be primarily associated with one specific physical cause. However because of the interactions between different physical mechanisms, an individual mode, whilst predominantly reflecting one physical mechanism, may nonetheless contain components from other mechanisms.
b) The higher (less energetic modes) are likely to be significantly affected by experimental variability, particularly for the full scale data considered here.
c) The effects of a finite number of sampling points and of experimental error are likely to be significant for, very approximately, the 50% of the modes with the lowest energy

Whatever one concludes concerning the physical nature of the POD modes, it seems to the author that the characteristic of POD that is most useful is the ability to represent the fluctuating pressure field on the surface of a structure through a relatively short series of terms. In particular pressure coefficient spectra can be expressed as series of the modal spectra. When applied to calculating extreme loads, ventilation rates etc, this results in simple straightforward expressions that are simple to use. If in addition one accepts that the modes represent physical mechanisms, such an approach also gives considerable physical insight into the physical phenomena involved.

Acknowledgements

The author would like to acknowledge the assistance of staff at Silsoe Research Institute who made available the full scale data used in this study.

References

Armitt, J. (1968), "Eigenvector analysis of pressure fluctuations on the West Burton Instrumented Cooling Tower", CEGB Report RD/LN114/68.

Baker, C.J. (1998), "The use of the technique of orthogonal modal decomposition in understanding the unsteady wind driven ventilation through buildings", *Proceedings WES Conference*, Bristol, UK.

Best, R.J., Holmes, J.D. (1983), "Use of eigenvalues in the covariance integration method for determination of wind load effects", *Journal of Wind Engineering and Industrial Aerodynamics*, **13**, 359-370.

Cherry, N., Hillier, R. and Latour, M. (1984), "Unsteady measurements in a separating and reattaching flow", *Journal of Fluid Mechanics*, **144**, 13-46.

Haghighat, F., Rao, J. and Fazio, P. (1991), "The influence of turbulent wind on air change rates - a modelling approach", *Building and Environment*, **26**(2), 95-109.

Holmes, J.D. (1990), "Analysis and synthesis of pressure fluctuations on bluff bodies using eigenvectors", *Journal of Wind Engineering and Industrial Aerodynamics*, **33**, 219-230.

Holmes, J.D., Sankaran, R., Kwok, K.C.S. and Syme, M.J. (1997), "Eigenvector modes of fluctuating pressure on low rise building models", *Journal of Wind Engineering and Industrial Aerodynamics*, **69-71**, 697-707.

Hoxey, R.P., Richards, P., Richardson, G.M., Robertson, A.P. and Short, J.L. (1995), "Silsoe Structures Building -

the completed experiment Part 2", *Proceedings* 9*th International Conference on Wind Engineering*, 1115-1126, Dehli, India.
Hoxey, R., Short, L. and Richards, P. (1999), "Quasi-steady theory developed with experimental verification", *Proceedings of the* 10*th International Conference on Wind Engineering*, Copenhagen, 1679-1686.
Kareem, A. and Cermak, J.E. (1984), "Pressure fluctuations on a square building model in boundary layer flows", *Journal of Wind Engineering and Industrial Aerodynamics*, **16**, 17-41.
Kikuchi, H., Tamura, Y., Ueda, H. and Hibi, K. (1997), "Dynamic wind pressures acting on a tall building model - proper orthogonal decomposition", *Journal of Wind Engineering and Industrial Aerodynamics*, **69-71**, 631-646.
Lee, B.E. (1975), "The effect of turbulence on the surface pressure field of a square prism", *Journal of Fluid Mechanics*, **69**, 263-282.
Letchford, C.W. and Mehta, K.C. (1993), "The distribution and correlation of fluctuating pressures on the Texas Tech building", *Journal of Wind Engineering and Industrial Aerodynamics*, **50**, 225-234.
Prevezer, T. (1998), "Wind pressure fluctuations on a low rise building", PhD thesis, University of Nottingham.
Prevezer, T., Baker, C.J. and Hoxey, R.P. (1997), "Unsteady pressure fluctuations on a low rise building", *Proceedings* 2*nd European Wind Engineering Conference*, Genoa.
Richardson, G., Hoxey, R., Robertson, A. and Short, J. (1995), "The Silsoe Structures Building. The completed experiment Part 1", *Proceedings* 9*th International Conference on Wind Engineering*, 1103-1114, Dehli, India.
Robertson, A.P., Hoxey, R.P., Short, J.L., Ferguson, W.A. and Blackmore, P.A. (1997), "Wind loads on boundary walls: Full scale studies", *Journal of Wind Engineering and Industrial Aerodynamics*, **69-71**, 451-459.
Tamura, Y., Suganuma, S., Kikuchi, H. and Hibi, K. (1999), "Proper orthogonal decomposition of random wind pressure fields", *Journal of Fluids and Structures*, **13**, 1069-1095.
Tamura, Y., Ueda, H., Kikuchi, H., Hibi, K., Suganuma, S. and Bienkiewicz, B. (1995), "Proper orthogonal decomposition study of approach wind-building pressure correlation", *Proceedings* 9*th International Conference on Wind Engineering*, Dehli, 2115-2126.

(*Communicated by Giovanni Solari*)